

Earth and Space Science



RESEARCH ARTICLE

10.1029/2023EA002901

Key Points:

- Observation-based data sets enable synoptic spatio-temporal assessments of Arctic Ocean carbonate system parameters
- Re-analysis and satellite products predict total alkalinity with accuracies of $\sim 21 \mu\text{mol kg}^{-1}$
- Targeted in situ data collection is needed to fully exploit satellite observations in the Arctic to enable carbonate system monitoring

Supporting Information:

Supporting Information may be found in the online version of this article.

Correspondence to:

H. L. Green,
h.green2@exeter.ac.uk

Citation:

Green, H. L., Findlay, H. S., Shutler, J. D., Sims, R., Bellerby, R., & Land, P. E. (2023). Observing temporally varying synoptic-scale total alkalinity and dissolved inorganic carbon in the Arctic Ocean. *Earth and Space Science*, 10, e2023EA002901. <https://doi.org/10.1029/2023EA002901>

Received 27 MAR 2023
Accepted 9 NOV 2023





Author Contributions:

Conceptualization: Hannah L. Green, Helen S. Findlay, Jamie D. Shutler, Richard Bellerby, Peter E. Land
Data curation: Hannah L. Green, Peter E. Land
Formal analysis: Hannah L. Green
Funding acquisition: Helen S. Findlay, Jamie D. Shutler, Richard Bellerby, Peter E. Land
Investigation: Hannah L. Green
Methodology: Hannah L. Green, Jamie D. Shutler, Richard Sims, Peter E. Land

© 2023 The Authors. Earth and Space Science published by Wiley Periodicals LLC on behalf of American Geophysical Union.

This is an open access article under the terms of the [Creative Commons Attribution License](https://creativecommons.org/licenses/by/4.0/), which permits use, distribution and reproduction in any medium, provided the original work is properly cited.

Observing Temporally Varying Synoptic-Scale Total Alkalinity and Dissolved Inorganic Carbon in the Arctic Ocean

Hannah L. Green^{1,2} , Helen S. Findlay¹, Jamie D. Shutler² , Richard Sims², Richard Bellerby^{3,4,5} , and Peter E. Land¹ 

¹Plymouth Marine Laboratory, Plymouth, UK, ²University of Exeter, Penryn, Cornwall, UK, ³Norwegian Institute of Water Research, Bergen, Norway, ⁴East China Normal University, Shanghai, China, ⁵UCSI University, Kuala Lumpur, Malaysia

Abstract The long-term absorption by the oceans of atmospheric carbon dioxide is leading to the slow decline of ocean pH, a process termed ocean acidification (OA). The Arctic is a challenging region to gather enough data to examine the changes in carbonate chemistry over sufficient scales. However, algorithms that calculate carbonate chemistry parameters from more frequently measured parameters, such as temperature and salinity, can be used to fill in data gaps. Here, these published algorithms were evaluated against in situ measurements using different data input types (data from satellites or in situ re-analysis climatologies) across the Arctic Ocean. With the lowest uncertainties in the Atlantic influenced Seas (AiS), where re-analysis inputs achieved total alkalinity estimates with Root Mean Squared Deviation (RMSD) of $21 \mu\text{mol kg}^{-1}$ and a bias of $2 \mu\text{mol kg}^{-1}$ ($n = 162$) and dissolved inorganic carbon RMSD of $24 \mu\text{mol kg}^{-1}$ and bias of $-14 \mu\text{mol kg}^{-1}$ ($n = 262$). AiS results using satellite observation inputs show similar bias but larger RMSD, although due to the shorter time span of available satellite observations, more contemporary in situ data would provide further assessment and improvement. Synoptic-scale observations of surface water carbonate conditions in the Arctic are now possible to monitor OA, but targeted in situ data collection is needed to enable the full exploitation of satellite observation-based approaches.

Plain Language Summary The long-term absorption by the oceans of atmospheric carbon dioxide is leading to the slow decline of ocean pH, a process termed ocean acidification (OA). Sea surface salinity and temperature measurements from satellites or in situ re-analysis products can be used as input to empirical algorithms to calculate OA parameters. This paper provides a first analysis of published Arctic Ocean empirical algorithms to estimate surface water OA parameters using observation-based data sets. Results show promise in the Atlantic influenced Seas using *both* in situ re-analysis and satellite products, but satellite salinity is relatively recent, and a paucity of in situ data in the satellite salinity era precludes a robust assessment. To fully exploit satellite-based approaches, efforts need to focus on collecting in situ data while these satellites are overhead and operating in orbit.

1. Introduction

The marine carbonate system is changing due to the absorption of CO_2 into the ocean from the atmosphere; approximately 26% of anthropogenic CO_2 emissions are absorbed by the oceans annually (Friedlingstein et al., 2021). Absorption of atmospheric CO_2 is changing the carbonate chemistry of the ocean, by increasing H^+ ions (decrease in pH) and decreasing carbonate ions and calcium carbonate mineral saturation states. This process is known as ocean acidification (OA) (Caldeira & Wickett, 2003).

In a recent paper by Qi et al. (2022) OA was observed to be happening at a rate four times faster than in other ocean basins in the Western Arctic Ocean. The Arctic Ocean is particularly susceptible to OA due to its low buffering capacity and freshening from river run off, glacial and sea ice melt (Bellerby, 2017; Bellerby et al., 2018; Jones et al., 2021; Krasting et al., 2022; Zhang et al., 2020). Corrosive saturation states for aragonite, a key calcium carbonate mineral for shell building organisms, are already being observed in the Chukchi and Laptev Seas (Cross et al., 2018), the Chukchi Sea and Beaufort Gyre region (Qi et al., 2017, 2022), Canadian Basin (Jutterström & Anderson, 2010), the central Arctic (CA) Ocean (Ulfsbo et al., 2018) and the Eastern Siberian sea (Anderson et al., 2011; Semiletov et al., 2016).

OA is just one of many climate driven changes impacting the Arctic Ocean, changes which, interact and influence the carbonate chemistry in a multitude of ways resulting in regional differences. Increased warming has led to

Project Administration: Hannah L. Green, Helen S. Findlay, Jamie D. Shutler, Peter E. Land
Software: Hannah L. Green, Richard Sims
Supervision: Helen S. Findlay, Jamie D. Shutler, Richard Bellerby, Peter E. Land
Validation: Hannah L. Green
Visualization: Hannah L. Green
Writing – original draft: Hannah L. Green
Writing – review & editing: Helen S. Findlay, Jamie D. Shutler, Richard Sims, Richard Bellerby

increased snow and glacial melting, resulting in increased river discharge and freshwater inputs into the Arctic Ocean (Shiklomanov et al., 2021; Solomon et al., 2021). The increase in freshwater content of the Arctic Ocean affects the carbonate chemistry by lowering total alkalinity (TA), and hence reducing the buffering capacity of the ocean (Pogojeva et al., 2022). However, if the freshwater input contains dissolved glacial bedrock high in carbonate minerals this can have the opposite effect, of increasing TA (Brown et al., 2020; Geilfus et al., 2021). Opposite to other Arctic regions, in the Barents Sea a decline in freshwater input has been observed, which has been linked to a decline in sea ice import into the region (Lind et al., 2018) and the progression of warmer, more saline Atlantic water which flows from the North Atlantic into the Arctic Ocean in a process that has been termed “Atlantification” (Polyakov et al., 2017).

Another resultant impact of warming is a reduction in sea ice cover and thickness (Kwok, 2018), which affects the complex interactions with surface carbonate chemistry and leads to a greater area for CO₂ gas exchange. This loss of sea ice cover is also impacting primary production (Wassmann et al., 2006), high primary productivity in the late spring and summer removes CO₂ from the water, while high respiration in the winter has the opposite effect (Semiletov et al., 2007). Collectively, these complex interactions and varying conditions result in changes in carbonate chemistry within Arctic waters that are highly regionally and temporally dependent and not well characterized, so effective monitoring is critical. Understanding and quantifying how the carbonate chemistry is changing in the Arctic Ocean will better inform the scientific community on how ecosystems, habitats, and species may be impacted by OA (Green et al., 2021).

Carbonate chemistry measurements traditionally have been collected as discrete samples on ship cruises, and more recently using sensors on Bio-Argo floats, moorings and other autonomous platforms that utilize sensors (Boutin et al., 2021b). Marine carbonate chemistry can be characterized using temperature, salinity, and any combination of two of the four variables: TA; dissolved inorganic carbon (DIC); pH; and partial pressure of carbon dioxide (*p*CO₂) (Dickson et al., 2007). TA and DIC have historically been measured using bottle sampling with laboratory analysis (Dickson et al., 2007). Historically for sea surface salinity (herein referred to as salinity) and sea surface temperature (herein referred to as temperature) have more routinely been measured than carbonate system parameters. The possibility of calculating TA and DIC from other oceanographic variables, such as salinity, oxygen, silicate, phosphate, and nitrate in the North Atlantic was first demonstrated by Brewer et al. (1995). This offered the potential of filling carbonate chemistry data set gaps through using more readily available data for example, satellite record and more frequently measured on hydrographic cruises and sensors. Following on from Brewer et al. (1995), the next stage was to establish algorithms for different oceans which Millero et al. (1998) began to develop. Lee et al. (2000) developed DIC algorithms further by producing algorithms for several ocean basins using temperature and nitrate. And Lee et al. (2006) developed algorithms to calculate the temperature and salinity relationship with TA using an optimal polynomial fit, dividing the global oceans up into five regions.

The first regional Arctic Ocean specific algorithm was developed by Tait et al. (2000) for the Labrador Sea, which used a multiple linear regression to calculate TA from salinity and temperature. Other studies derived simple linear regression algorithms between salinity and TA for other Arctic Ocean regions, including the Barents Sea (Kaltin et al., 2002), CA Ocean and Kara and Laptev Seas (Fransson et al., 2001), the North Pacific (Wong et al., 2002), Norwegian Sea (Bellerby et al., 2005) and Chukchi Sea (Kaltin & Anderson, 2005). These advances were followed by Arrigo et al. (2010) who developed multiple linear regression for both TA and DIC for Barents and Greenland Seas; whilst Takahashi et al. (2014) also used a multiple linear regression to develop TA algorithms for six regions in the Arctic Ocean.

All of these approaches used in situ or modeled data for salinity and temperature inputs. The potential of using satellite observations to observe the carbonate system via the same empirical algorithms was identified by Land et al. (2015) and Salisbury et al. (2015). Although to date only a few studies have attempted to use satellite data as inputs for TA or DIC empirical algorithms (Fine et al., 2017; Gregor & Gruber, 2021; Land et al., 2019; Sims et al., 2023). These global and regional approaches show much promise (e.g., root mean square difference of 17 μmol kg⁻¹; Land et al., 2019). However, none of these studies have addressed polar waters and the full potential of satellite observations for studying ocean carbon remains largely unexplored (Shutler et al., 2020).

Early work by Swift and McIntosh (1983) and Yueh et al. (2001) identified how salinity can be determined from satellite observed emissivity and its relationship with conductivity (e.g., in a similar way to how in situ instruments relate conductivity to salinity). These salinity data sets are now routinely provided by the following

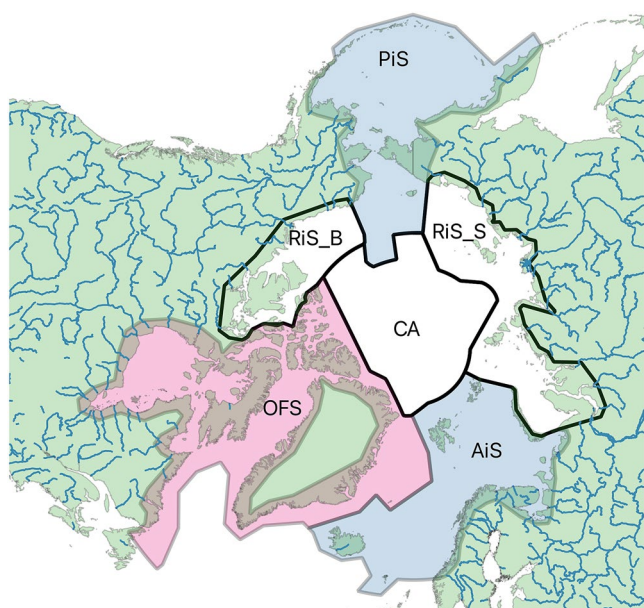


Figure 1. The different biogeochemical regions being studied. AiS, Atlantic influenced Seas; OFS, Outflow Seas; PiS, Pacific influenced Seas; RiS_B, River influenced Seas- Beaufort Sea; RiS_S, River influenced Seas- Siberian seas; CA, central Arctic. Highlighted in blue are the inflow shelves and highlight in pink are the outflow shelves. Blue line on map are rivers. Made with Natural Earth (Patterson & Vaughn Kelso, 2023).

satellites platforms or sensors: the Soil Moisture and Ocean salinity (SMOS) satellite; the Aquarius sensor on board the SAC-D spacecraft; and the Soil Moisture Active Passive (SMAP) satellite (Vinogradova et al., 2019). The careful inter- and cross-calibration between these different observations, has enabled the generation of a multi-sensor temporally consistent global coverage climate data record with well-characterized uncertainties that is monitored and continues to be updated with new data (combined uncertainties of 0.15 when compared to global Argo data, Boutin et al., 2021a). Equivalent inter- and cross-calibrated multi-sensor data product specific to the high latitudes has also been produced (combined uncertainties of 0.24–0.35 when compared to Argo; Olmedo et al., 2018) and its development highlighted the lack of in situ data available in some polar regions. Satellite observed temperature data can be used to calculate DIC and TA and global satellite-observed climate data records with well characterized uncertainties are available for these parameters as well (Merchant et al., 2019). Satellite observed chlorophyll-a (chl a) concentration can also be used in empirical relationships to calculate DIC (Sathyendranath et al., 2019). Additionally, the development of re-analysis data sets and large community data set collation and quality control activities means that other large in situ or observation-based data sets are now available (Cabanes et al., 2013; Kolodziejczyk, Hamon, et al., 2021; Szekely, Gourrion, Pouliquen, & Reverdin, 2019).

The objective of this work was to evaluate the published empirical algorithms with different combinations of input data sources to drive the regional calculations of alkalinity and DIC. And to then evaluate whether in situ re-analysis products and satellite observations can be robustly used in the Arctic Ocean as a method for monitoring surface carbonate chemistry and hence evaluating OA and its impacts.

2. Materials and Methods

2.1. Data

2.1.1. Study Area

The Arctic Ocean was separated into six biogeochemical regions based on previous work by Carmack and Wassmann (2006) and following Findlay et al. (2015) and as guided by Green et al. (2021) giving: the inflow shelves of the Atlantic influenced seas (AiS) and Pacific influenced seas (PiS); the river influenced seas (RiS) can be separated into two areas: the east Arctic along the Siberian coast (RiS_S) which encompasses: Kara Sea; Laptev Sea; East Siberian Sea, and then the Beaufort Sea (RiS_B); the CA; and the outflow shelves (OFS) of the Canadian Arctic and East Greenland (Figure 1).

2.2. Analysis of Published Algorithms

A total of 23 TA and 5 DIC studies publishing Arctic specific regional algorithms using a selection of temperature, salinity, chlorophyll-a, and nitrate (NO_3^-) as input data were analyzed (Tables S1 and S2 in Supporting Information S1). While these algorithms have been developed and used with in situ data and climatologies to calculate DIC and TA, optimal assessment of spatially complete in situ re-analysis data or satellite observations (Table 1), to calculate both DIC and TA in the Arctic Ocean have yet to be assessed.

Each algorithm was analyzed using a combination of input data sources (Table 1). Every input combination for each algorithm was evaluated. The methodology within Land et al. (2019) and an in situ versus satellite data matchup database “OceanSODA-MDB” (Land et al., 2023) was used to evaluate and rank DIC and TA algorithm-input combinations in the Arctic Ocean, allowing the algorithm-input combination with the lowest uncertainties to be identified for each region. Limiting the minimum number of estimates versus in situ matchups to $n \geq 30$ was chosen to identify the most robust choices (Sims et al., 2023), but all results irrespective of n were

Table 1

The Different Input Data Sets Used in the Algorithm Comparison From Land et al. (2023) OceanSODA-MDB (Satellite Oceanographic Data Sets for Acidification)

Name	Parameters	Information	Reference
European Space Agency Climate Change Initiative the Operational Sea Surface Temperature and Sea Ice Analysis v2. (ESACCI temperature)	Temperature	Satellite observations	Good et al. (2019, 2020) and Merchant et al. (2019)
Optimum Interpolation Sea Surface Temperature v2.1 (OItemperature)	Temperature	Gridded data from satellites, ships, buoys, and Argo floats	Banzon et al. (2016) and Huang et al. (2021)
Coriolis Ocean database for Reanalysis v5.2 (CORA)	Temperature Salinity	Global ocean- gridded in-situ observations	Szekely, Gourrion, Pouliquen, Reverdin, and Merceur (2019)
Remote Sensing Systems National Aeronautics and Space Administration Soil Moisture Active Passive v4.0 (SMAP)	Salinity	Satellite observations	Meissner and Wentz (2019)
European Space Agency Climate Change Initiative Sea Surface Salinity v2.31 (ESACCI salinity)	Salinity	Satellite observations	Boutin et al. (2021a)
In Situ Analysis System 15 (ISAS)	Salinity	Gridded data from Argo, Moorings, Marine Mammals, merchant ships	Kolodziejczyk, Prigent-Mazella, and Gaillard (2021)
World Ocean Atlas (WOA)	NO ₃ ⁻ , PO ₄ ³⁻ , SiO ₄ ⁴⁻ , O ₂	In situ profile data	Boyer et al. (2018)
European Space Agency Climate Change Initiative Ocean color	Chl a	Satellite observations	Sathyendranath et al. (2019)
Barcelona Expert Center Soil Moisture and Ocean Salinity high latitude (BEC Arctic salinity)	Salinity	Satellite observations	Olmedo et al. (2018)

Note. Temperature, sea surface temperature; Salinity, sea surface salinity; Chl a, chlorophyll a; DO, dissolved oxygen; NO₃⁻, nitrate; PO₄³⁻, phosphate; SiO₄⁴⁻, silicate; DIC, dissolved inorganic carbon; TA, total alkalinity.

still analyzed. Weighted Root Mean Squared Deviation (RMSD) and weighted bias statistics (e.g., as used by Ford et al., 2021) were used to evaluate all uncertainties and these represent a Type A uncertainty analysis following the guidelines of the International Bureau of Weights and Measures (BIPM, 2008). The weights ensure that the uncertainties from the original algorithm and in situ uncertainties are included within the analysis. Weights were derived from the sum of the individual weight of each algorithm (w), where:

$$w = \frac{1}{\sqrt{((\text{literature algorithm uncertainty})^2 + (\text{in situ measurement uncertainty})^2)}$$

Algorithms without a published algorithm uncertainty could not be included in the weighted statistics (as they lack the required model uncertainty value) and hence were not included in the final evaluation. Only algorithm-input combinations with 30 or more in situ matchups ($n \geq 30$) were considered where this was possible, but combinations with $n < 30$ were included otherwise.

3. Results

Here we present the overall results from the $n \geq 30$ evaluation and then the satellite data driven algorithm-input combinations where $n < 30$ are presented.

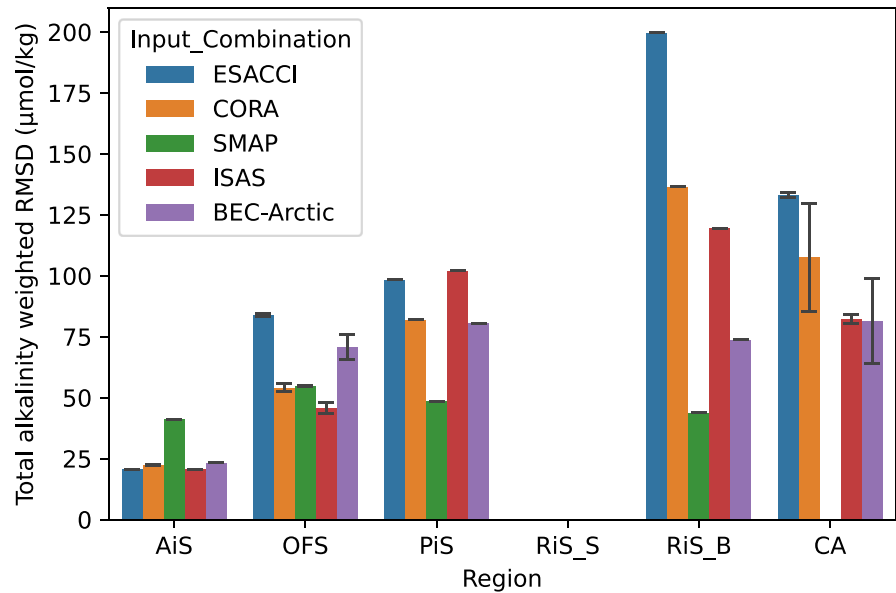
3.1. Total Alkalinity

3.1.1. Atlantic Influenced Seas

The salinity-TA relationships were most effective in the AiS, having the lowest RMSD of all the regions. The algorithm-input combination with the lowest combined uncertainties was Nondal et al. (2009) using the ISAS data set (RMSD 20.7 and bias 2.3 $\mu\text{mol kg}^{-1}$, $n = 162$, Figures 2 and 3, Table S3 in Supporting Information S1). Algorithm-CORA combination also had low combined uncertainties in this region (RMSD 22.5 and bias 3.4 $\mu\text{mol kg}^{-1}$, $n = 191$, Figure 2, Table S3 in Supporting Information S1).

None of the satellite data set matchups had $n \geq 30$; both algorithm-ESACCI combinations (RMSD 20.7 and bias 9.1 $\mu\text{mol kg}^{-1}$, $n = 16$, Table S3 in Supporting Information S1) and algorithm-BEC Arctic combinations

A



B

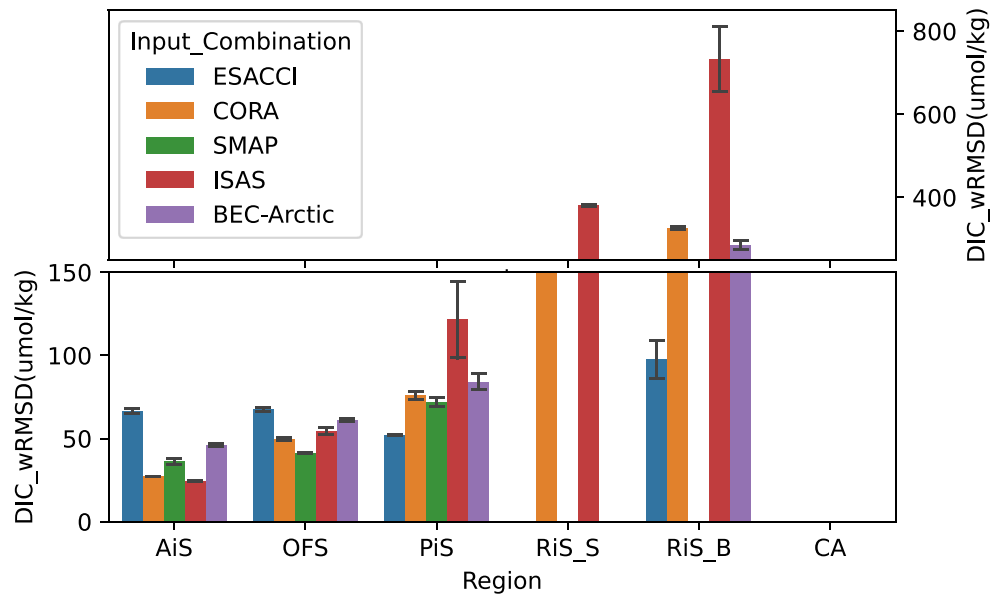
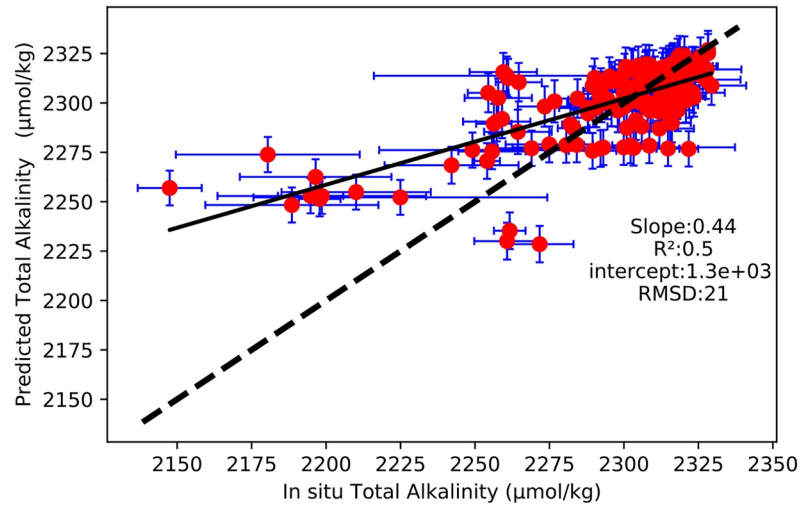


Figure 2. The mean weighted RMSD output for each salinity source, data grouped by region and salinity source. (a) Total alkalinity, (b) dissolved inorganic carbon. Error bars represent the standard deviations for the mean RMSD for that salinity input combinations.

(RMSD 23.4 and bias $-4.0 \mu\text{mol kg}^{-1}$, $n = 19$, Table S3 in Supporting Information S1) uncertainties were comparable to the reanalysis products. However, algorithm-SMAP combination had high combined uncertainties in comparison (RMSD 41.1 and bias $28.1 \mu\text{mol kg}^{-1}$, $n = 8$, Table S3 in Supporting Information S1). The standard deviation (SD) of the in situ data for this region was $38 \mu\text{mol kg}^{-1}$ (Table S4 in Supporting Information S1; calculated from the regional in situ data of Land et al., 2023) and hence the algorithm-ESACCI and BEC Arctic combinations are both accurate enough to distinguish natural variations in TA when applied to the AiS region.

A



B

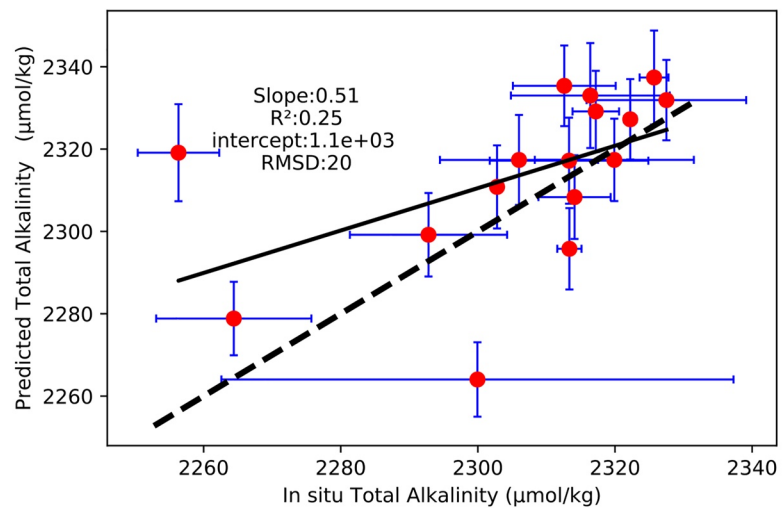


Figure 3. The lowest uncertainty algorithm-input combination outputs compared against in situ for Atlantic influenced Seas for re-analysis products and satellite. (a) Predicted total alkalinity (TA) using ISAS salinity input data set with Nondal et al. (2009) algorithm against in situ TA. (b) Predicted TA using the lowest uncertainty satellite salinity algorithm-input combination, ESACCI Soil Moisture and Ocean salinity with Nondal et al. (2009) algorithm against in situ TA. (c) Predicted dissolved inorganic carbon (DIC) using the lowest uncertainty algorithm-input reanalysis combination with ISAS salinity and ESACCI temperature with Nondal et al. (2009) algorithm against in situ DIC. (d) Predicted DIC using Soil Moisture Active Passive salinity and CORA temperature with Nondal et al. (2009) algorithm against in situ DIC. The X error bars are the TA reference output uncertainty, and the y error bars are the predicted combined output uncertainty. Solid black line is the regression line of in situ TA against calculated TA and the dashed line is $y = x$. Note the axis are on difference scales.

3.1.2. Pacific Influenced Seas

The Kaltin and Anderson (2005) algorithm-BEC Arctic combination had the lowest uncertainties in the PiS (RMSD 80.6 and bias 28.9 $\mu\text{mol kg}^{-1}$, $n = 39$; Figure 2 and Figure S3 in Supporting Information S1, Table S5 in Supporting Information S1). The algorithm-ISAS and CORA combinations had higher combined uncertainties (RMSD 89.5 and 81.2 $\mu\text{mol kg}^{-1}$; bias -5.6 and 4.9 $\mu\text{mol kg}^{-1}$; $n = 196$ and 223, respectively; Figure 2, Table S5 in Supporting Information S1), although RMSDs are less than the SD of the region (108 $\mu\text{mol kg}^{-1}$; Table S4 in Supporting Information S1). Neither the algorithm-SMAP nor ESACCI combinations had matchups with $n \geq 30$, however, algorithm-SMAP combination came close and had lowest combined uncertainties

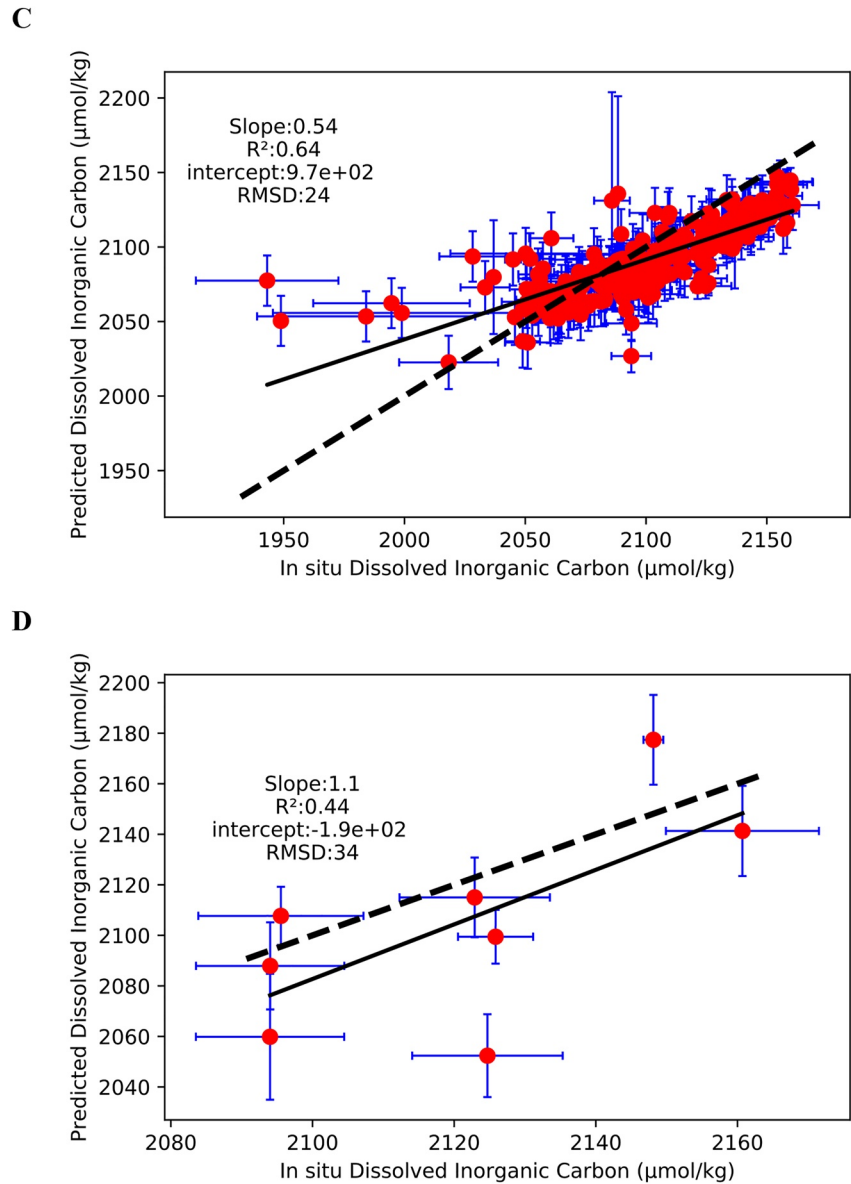


Figure 3. (Continued)

of all data sets (RMSD 48.5 and bias $21.10 \mu\text{mol kg}^{-1}$, $n = 26$, Table S3 in Supporting Information S1). ESACCI had high combined uncertainties (RMSD 98.3 and bias $58.4 \mu\text{mol kg}^{-1}$, $n = 8$, Table S3 in Supporting Information S1).

3.1.3. Outflow Shelf

The Tynan et al. (2016) algorithm-ISAS salinity and CORA temperature input data set combinations in OFS had the lowest combined uncertainties (RMSD $43.0 \mu\text{mol kg}^{-1}$, $n = 223$, Figure 2 and Figure S3 in Supporting Information S1). The algorithm-CORA salinity combinations had higher uncertainties, with the lowest combined uncertainties with CORA temperature (RMSD $51.8 \mu\text{mol kg}^{-1}$, $n = 357$, Table S5 in Supporting Information S1). The algorithm-SMAP combinations had the lowest combined uncertainties (RMSD $54.6 \mu\text{mol kg}^{-1}$, $n = 24$, Table S3 in Supporting Information S1). For all algorithm-ESACCI and BEC Arctic salinity inputs combinations produced higher RMSDs (RMSD $83.3 \mu\text{mol kg}^{-1}$ and $67.0 \mu\text{mol kg}^{-1}$; bias $39.8 \mu\text{mol kg}^{-1}$ and $20.6 \mu\text{mol kg}^{-1}$; $n = 50$ and 71 , respectively, Figure 3, Table S5 in Supporting Information S1) than the SD of TA in the region ($68 \mu\text{mol kg}^{-1}$; Table S4 in Supporting Information S1).

3.1.4. River Influenced Seas

RiS_B had a greater number of data points in the OceanSODA-MDB than RiS_S, with a total of 372 matchups for TA. The DeGrandpre et al. (2019) algorithm-BEC Arctic salinity combination produced the lowest uncertainties with $n > 30$ (RMSD 73.8 and bias 24.0 $\mu\text{mol kg}^{-1}$, $n = 50$, Figure 2 and Figure S3 in Supporting Information S1 & Table S5 in Supporting Information S1). The algorithm-CORA and ISAS combinations RMSDs (RMSD 136.5 and 119.4 $\mu\text{mol kg}^{-1}$, bias 52.3 and 8.3 $\mu\text{mol kg}^{-1}$, $n = 161$ and 98, respectively; Table S5 in Supporting Information S1) were also above the SD for the region (SD = 131 $\mu\text{mol kg}^{-1}$, Table S4 in Supporting Information S1). The algorithm-SMAP combination has the lowest uncertainties out of all data sets but with low n number (RMSD 43.1 $\mu\text{mol kg}^{-1}$, bias = -9.9 $\mu\text{mol kg}^{-1}$, $n = 17$, Table S3 in Supporting Information S1). The algorithm-ESACCI combinations had higher uncertainties in comparison (RMSD 199.7 $\mu\text{mol kg}^{-1}$, bias 179.6 $\mu\text{mol kg}^{-1}$, $n = 25$, Table S3 in Supporting Information S1).

3.1.5. Central Arctic

The Arrigo et al. (2010) algorithm-ISAS salinity combination had lowest uncertainties in the CA (RMSD 79.6 $\mu\text{mol kg}^{-1}$, bias -6.7 $\mu\text{mol kg}^{-1}$, $n = 256$, Figure S3 in Supporting Information S1), and had lower SD of the in situ data for this region (SD 131 $\mu\text{mol kg}^{-1}$, Table S4 in Supporting Information S1). The algorithm-CORA combinations had higher combined uncertainties in comparison (RMSD 91.9 $\mu\text{mol kg}^{-1}$, bias 29.5 $\mu\text{mol kg}^{-1}$, $n = 175$, Figure S3 in Supporting Information S1). No SMAP matchups were identified. Both algorithm-ESACCI and BEC Arctic combinations had low n (RMSD 132.1 and 56.9 $\mu\text{mol kg}^{-1}$; bias -3.4 and 8.3 $\mu\text{mol kg}^{-1}$; $n = 8$ and 18, respectively, Table S3 in Supporting Information S1) but Arrigo et al. (2010) algorithm-BEC Arctic combination had lowest uncertainties out of all input combinations.

3.2. Dissolved Inorganic Carbon

The section below presents and discusses the DIC algorithm-input combinations, as with the section above, we first report the results of the $n \geq 30$ results and then results from the $n < 30$. There were no matchups for the CA region.

3.2.1. Atlantic Influenced Seas

As with TA, the AiS region was found to have the lowest combined uncertainties. The algorithm Nondal et al. (2009) with ISAS salinity and ESACCI temperature data sets had the lowest combined uncertainties (RMSD 24.4 and bias -13.9 $\mu\text{mol kg}^{-1}$, $n = 262$, Figures 2 and 3). The algorithm-CORA combinations had higher uncertainties (RMSD 27.2 and bias -14.7 $\mu\text{mol kg}^{-1}$, $n = 360$, Table S6 in Supporting Information S1). Similar to TA, no satellite salinity data sets had $n \geq 30$, this due to only a few in situ data points in OceanSODA-MDB in AiS in the time frame of satellite salinity. Satellites salinity algorithm-input combination RMSDs were much higher, with SMAP algorithm-input combination with the lowest combined uncertainty out of all satellite data sets (RMSD 33.8 and bias -17.8 $\mu\text{mol kg}^{-1}$, $n = 8$, Table S7 in Supporting Information S1). The algorithm-BEC Arctic and ESACCI combinations had higher uncertainties (RMSD 45.1 and 64.8 $\mu\text{mol kg}^{-1}$; bias -31.8 and -46.3 $\mu\text{mol kg}^{-1}$; $n = 43$ and 44, respectively, Table S6 in Supporting Information S1).

3.2.2. Pacific Influenced Seas

The Lee et al. (2000) algorithm with the OI (Optimum Interpolation) Temperature and CORA salinity combinations had the lowest uncertainty for the PiS (RMSD = 74.3 $\mu\text{mol kg}^{-1}$, bias -34.9 $\mu\text{mol kg}^{-1}$, $n = 137$; Figure 2 and Figure S3 in Supporting Information S1, Table S6 in Supporting Information S1). The algorithm-ISAS salinity combinations had higher RMSD and bias (RMSD 88.9 $\mu\text{mol kg}^{-1}$, bias 62.9 $\mu\text{mol kg}^{-1}$, $n = 142$; Figure 2, Table S6 in Supporting Information S1). The SD for DIC in this region was 98 $\mu\text{mol kg}^{-1}$ (Table S4 in Supporting Information S1), all CORA salinity combinations were below this. In this region satellite salinity data sets $n < 30$, though all algorithm-satellite salinity combinations uncertainties were below the SD for the region. ESACCI salinity combinations had the lowest combined uncertainties out of the salinity data sets but had a very low n value (RMSD 52.0 $\mu\text{mol kg}^{-1}$, bias -41.5 $\mu\text{mol kg}^{-1}$, $n = 5$; Figure 2, Table S7 in Supporting Information S1). The algorithm-SMAP and BEC Arctic combinations had a lower bias than the re-analyzed products (RMSD 68.9 $\mu\text{mol kg}^{-1}$, RMSD 77.8 $\mu\text{mol kg}^{-1}$, bias -32.7, -25.1 $\mu\text{mol kg}^{-1}$; $n = 12$, 11, respectively; Table S7 in Supporting Information S1).

3.2.3. Outflow Shelf

The Nondal et al. (2009) algorithm-CORA salinity combination had the lowest combined uncertainties with $n > 30$ (RMSD $48.6 \mu\text{mol kg}^{-1}$, bias $-4.3 \mu\text{mol kg}^{-1}$, $n = 309$; Figure 2 and Figure S3 in Supporting Information S1, Table S6 in Supporting Information S1). The algorithm-ISAS combinations had a much higher bias and RMSD (RMSD $52.6 \mu\text{mol kg}^{-1}$, bias $-28.1 \mu\text{mol kg}^{-1}$, $n = 204$, Table S6 in Supporting Information S1). Satellites algorithm-input combinations had the highest match ups in this region with in situ DIC. Both BEC Arctic and ESACCI salinity data sets with Lee et al. (2000) algorithm-input combination reaching over our n threshold had higher combined uncertainty than re-analysis products (RMSD $60.8, 67.7 \mu\text{mol kg}^{-1}$; bias $-5.2, 1.6 \mu\text{mol kg}^{-1}$; $n = 70, 66$, respectively, Table S6 in Supporting Information S1). The algorithm-SMAP salinity combination had lowest RMSD, though n was less than 30 (RMSD $41.1 \mu\text{mol kg}^{-1}$, bias $19.3 \mu\text{mol kg}^{-1}$, $n = 23$, Table S7 in Supporting Information S1).

3.2.4. River Influenced Seas

There were no match ups with $n \geq 30$ for analysis in the RiS_S region, and no satellite match ups. Lee et al. (2000) algorithm-CORA and ISAS combination had lowest combined uncertainty (RMSD $236.8, 377.9 \mu\text{mol kg}^{-1}$; bias $100.7, -242.1 \mu\text{mol kg}^{-1}$, $n = 27, 28$; respectively; SD $271 \mu\text{mol kg}^{-1}$; Table S4 in Supporting Information S1). This region needs more data and regionally tuned algorithm development.

The RiS_B had sufficient data, but algorithm-input combination had high uncertainties. The Arrigo et al. (2010) algorithm with CORA salinity and OI temperature combination with $n > 30$ had the lowest combined uncertainties (RMSD $335.9 \mu\text{mol kg}^{-1}$, bias $-26, 5 \mu\text{mol kg}^{-1}$, $n = 64$; Figure 2 and Figure S3 in Supporting Information S1, Table S6 in Supporting Information S1). The algorithm-ISAS combination produced very large bias and RMSD, with the lowest RMSD and bias much higher (RMSD $623.7 \mu\text{mol kg}^{-1}$, bias $-668.5 \mu\text{mol kg}^{-1}$, $n = 89$, Table S6 in Supporting Information S1). The algorithm-ESACCI combinations had lowest uncertainties out of all salinity combinations but very low n value (RMSD $81.4 \mu\text{mol kg}^{-1}$, bias $26.8 \mu\text{mol kg}^{-1}$, $n = 6$, Table S7 in Supporting Information S1). There were no SMAP matchups. The algorithm-BEC Arctic combinations had lower uncertainties than algorithm-ISAS combination (RMSD $269.5 \mu\text{mol kg}^{-1}$, bias $-181.0 \mu\text{mol kg}^{-1}$, $n = 24$, Table S7 in Supporting Information S1).

4. Discussion

This work has demonstrated that for some regions of the Arctic Ocean, satellite or reanalysis data can be used as input data sets to algorithms in order to calculate DIC and TA with uncertainty that matches the variability seen in situ data. In other regions some algorithms and input combinations had higher uncertainties. Here we discuss possible reasons for these differences and make recommendations for future development.

4.1. Atlantic Influenced Seas

The TA algorithm-input combinations had lower uncertainties in the AiS than all other regions. Furthermore, the RMSDs found here using the Nondal et al. (2009) algorithm were much higher than those reported by Nondal et al. (2009) (RMSD $6.2 \mu\text{mol kg}^{-1}$ and bias $-1.8 \mu\text{mol kg}^{-1}$). There could be several explanations for these results; there are fewer TA in situ data for the most recent decade, and within the OceanSODA-MDB (Figure S1 in Supporting Information S1), to analyze uncertainties in this region. For example, PiS has a lot more TA matchups in the satellite time period year 2010–2020 than AiS. The region is also undergoing rapid change; for example, rapid warming is occurring in the Barents Sea, with winter warming rates more than twice the rate of warming in other Arctic areas, and with a decadal trend of 1.74°C of warming (Cai et al., 2022). Warming has led to sea ice loss in the Barents Sea with a reduction in ice extent by two thirds since 1979 (Onarheim & Årthun, 2017).

The region is also subject to measurable acidification, the Ocean Weather Station M based in the AiS has recorded a decrease in surface pH of -0.092 and an increase in the surface by $2.92 \pm 0.37 \mu\text{atm year}^{-1}$, over the last 28 years (Skjelvan et al., 2022). The freshwater and salinity budget are also changing. In the Nordic Seas there has been considerable decrease in freshwater content of the area and TA has been observed to be increasing from 1981 to 2019 (Fransner et al., 2022). There is also evidence of “Atlantification” a process whereby warmer, saltier Atlantic water is moving further north into the AiS region of the Arctic than was previously

occurring. Atlantification has led to changes in species distribution, this can have an impact on carbonate chemistry, for example, the northward expansion of calcifying *Emiliana Huxleyi* impacts the carbonate chemistry of the surrounding water column by decreasing TA in the growth season and increasing TA when *E. Huxleyi* decay (Oziel et al., 2020; Robertson et al., 1994). Hence, Atlantification can impact carbonate chemistry algorithms in two main ways: the first being that Atlantic water has higher salinity and warmer temperature (Arrigo et al., 2010) so the algorithms are different for TA and DIC. The second being influx of calcifying *E. Huxleyi* that decrease TA and therefore also changes the relationship between salinity and TA. The Nondal et al. (2009) algorithm, although has low combined uncertainties, was trained on data well over a decade old and therefore may be less likely to predict more recent changes in the salinity-TA relationship in this region. More recent in situ TA data is needed to test this. Thus, climate change consequences seen in recent years since these older algorithms were developed highlights the potential need for algorithm retraining and addition of modern in situ TA data.

For the DIC analysis, the Nondal et al. (2009) algorithm-input combinations had lower uncertainty in this region compared to the Arrigo et al. (2010) or Brewer et al. (1995) algorithm-input combinations. This reduced uncertainty is most likely due to Nondal et al. (2009) using two different algorithms to capture the seasonal effect on DIC. The CORA and ISAS input data sets with the Nondal et al. (2009) algorithm have RMSD well below the SD of DIC in this region (SD $43 \mu\text{mol kg}^{-1}$, Table S4 in Supporting Information S1). The recent changes in the region mentioned above could also be impacting the DIC algorithms, especially given, as with TA, there are fewer DIC data for recent years and within the OceanSODA-MDB (Figure S2 in Supporting Information S1). These results suggest algorithms need retuning to improve the uncertainties when using satellite inputs ESACCI salinity and BEC Arctic. At present, ESACCI salinity and BEC Arctic are not suitable to be used as input sources for published DIC algorithms. To support this, further efforts of DIC in situ data collection are needed.

4.2. Pacific Influenced Seas

The largest difference between the calculated TA and the in situ TA was close to the shelf break. The shelf break in this region is a known area of upwelling of deep Atlantic Water, which circulates across the Arctic Ocean from the AiS (Li et al., 2022). The deep Atlantic Water has a different salinity-TA relationship to Pacific Water (Arrigo et al., 2010), and may explain why the PiS-specific algorithms do not reproduce the TA values seen in situ. Sea ice formation and melt also affects the salinity-TA relationship by changing the y-intercept of the equation (MacGilchrist et al., 2014), and hence there is likely to be a seasonal salinity-TA signal, which is not explored in these published algorithms. Despite some algorithm-input data set combinations having high RMSD, the overall high variability in this region (SD $108 \mu\text{mol kg}^{-1}$) suggests it is still possible to use algorithms with satellite inputs to calculate TA.

Arrigo et al. (2010) developed two seasonal DIC relationships for the PiS region, with an RMSD of $17.3 \mu\text{mol kg}^{-1}$ in spring and $61.6 \mu\text{mol kg}^{-1}$ in summer, resulting in reduced uncertainties compared to other algorithm-input combinations. Kim et al. (2021) identified a strong relationship between DIC and salinity in two out of the three summers in their study period between the years 2016–2018. The results from Kim et al. (2021) suggested that biological activity on annual process impacted the DIC–salinity relationship. The Arrigo et al. (2010) algorithm used Chl a in the algorithm to calculate DIC which is a good proxy for biological activity and maybe why this algorithm derived DIC with the lowest uncertainty.

Overall algorithm–satellites salinity combinations had lower uncertainties than the algorithm-re-analysis salinity combinations. However, for all salinity algorithm-input combinations the RMSD and bias are large; to reduce these uncertainties other variables might need to be incorporated in to DIC algorithm that capture other processes affecting DIC such as vertical/lateral mixing. Future work in this region would benefit from integrating the use of satellites to detect upwelling events. Quilfen et al. (2021) demonstrated the use of satellites to detect upwelling along the coast of California. Combining satellite surface wind and upwelling analyses with satellite derived carbonate chemistry estimates could provide better synoptic monitoring for the carbonate system in these Arctic waters. Hence, while overall algorithm-satellites salinity combinations had lower uncertainties in comparison to the algorithm-re-analysis salinity combinations, further development of algorithms in this region is needed. As well as continued effort for DIC in situ sampling to increase the number of satellite matchups.

4.3. Outflow Shelf

The Tynan et al. (2016) algorithm-input combinations had the lowest uncertainties for this region, most likely due to the optimal polynomial fit of this relationship, which can capture the nuances of the complex regional dynamics.

Our results suggest that it is not yet possible to use algorithm-satellite salinity combinations in this region as the combinations had the highest uncertainties, however, TA can be estimated from algorithm-salinity re-analysis combinations. When the salinity in situ data were plotted against the three satellite inputs (Figure S4 in Supporting Information S1) there was a low matchup with the algorithm-BEC Arctic combination (slope = 0.54, $R^2 = 0.72$, Figure S4 in Supporting Information S1) and algorithm-ESACCI combination (slope = 0.72, $R^2 = 0.44$, Figure S4 in Supporting Information S1). This could suggest that the higher uncertainty of the satellite driven methods in this region are due to either a depth mismatch with respect to the in situ data, or sea ice contamination leading to greater uncertainties within these satellite data. Sea ice contamination can occur due to the signal from the ice influencing the signal that the satellite views, or considers, the ocean. The study of this complexity is an ongoing focus of research, and the satellite salinity community are continuing to work to improve the sea ice corrections in level 3 data sets (Kolodziejczyk, Hamon, et al., 2021).

All algorithm-salinity combinations had lower uncertainties than the SD for DIC in this region ($67 \mu\text{mol kg}^{-1}$; Table S4 in Supporting Information S1), except for ESACCI salinity with the ESACCI and OI temperature data sets (Table S7 in Supporting Information S1). The variability in DIC in the OFS caused by ice and glacial melt maybe one reason for higher uncertainties. A reduction in ice cover can lead to an increase in light availability, which in turn can increase primary production (Lewis et al., 2016) and ultimately impact DIC relationships (Arrigo et al., 2010). Beupr -Laperri re et al. (2020) observed that a third of all changes in DIC throughout the season are as result of biological activity, whereby primary producers consume DIC in surface waters during the summer months and mixing of remineralized organic matter contributes to increasing DIC in the winter (Mathis & Questel, 2013).

To further reduce the high bias it is likely that further algorithm development work is required with a larger in situ training data set for this very geographically-complex region. The OFS is a large region with high spatial variability both in geographic features, such as inlets between islands, circular bays, and rivers, but also processes that influence the salinity and carbonate system. Climate change is changing the processes and timings that control TA, for example, river input can decrease or increase TA depending on the composition of river water, while ice melting and formation also influence TA via changes in salinity but also from ikaite formation and dissolution (Nondal et al., 2009). Changes in these processes will affect the salinity-TA relationship, for example, water flowing through the OFS that has been diluted by ice melt will have a lower y-intercept value than polar water (Nondal et al., 2009). This makes the region very nuanced and with more availability of in situ data future work should investigate dividing OFS into smaller sub-regions for algorithm development, as large bays like Baffin Bay are likely to have different TA and DIC relationships to the smaller straits like Franklin Strait for example. However, currently there are not enough in situ data to investigate these complexities.

4.4. River Influenced Seas

RiS_S has historically been understudied; the matchup database only had 69 matches for TA in the region (Land et al., 2023; Table S4 in Supporting Information S1), and in weighted analysis there were no data points in the matchup database within the algorithm boundary parameters tested. Hence, we were not able to assess this region. The rivers that flow into the RiS_S have often a lower TA value than the ocean for example, Cooper et al. (2008) found the Ob' and Yenisey rivers had an average alkalinity of 1,518 and 1,047 $\mu\text{mol kg}^{-1}$. Considering the large change in input source composition over recent decades it is vital that we understand how this input from rivers is affecting the carbonate chemistry of this region. For instance, Drake et al. (2018) found that in the Yenisey and Ob' rivers TA export increased by 185% and 134% over a 41-year period, respectively. The Eastern Laptev Sea is already supersaturated with respect to $p\text{CO}_2$ and has been found to release CO_2 back into the atmosphere during the ice-free season instead of absorbing the CO_2 (Pipko et al., 2016). In 2012 a 30% increase in primary production compared to 1993 was observed in the Laptev Sea continental slope part of the RiS_S, this increase in primary production is thought to be related to ice formation happening later and ice melting happening earlier in the year leading to a shorter ice cover period (Bienhold et al., 2022). The increase in primary production is also likely to impact the carbonate chemistry of the surface waters. Further work is therefore urgently required for both collecting more in situ data and developing regional algorithms for the RiS_S.

The dynamics of the RiS linked to high TA variability (Cooper et al., 2008; Findlay et al., 2015), large river outflows modified by permafrost, precipitation and primary production (Drake et al., 2018), sea ice loss (Yamamoto-Kawai et al., 2009) and variations in ground water inputs (Findlay et al., 2015), are potential reasons

for high uncertainty in RiS_B. The complex processes influence TA mean that a simple salinity-TA relationship will probably not characterize either RiS region with low uncertainty. As seen in the results for RiS_B TA algorithms have high uncertainty, however, to test this theory out in RiS_S more in situ data is needed. For algorithms to capture the nuances of RiS_B, they will have to be regionally tuned to capture the processes influencing TA in the region.

The SD for DIC in RiS_B was very large $105 \mu\text{mol kg}^{-1}$ (Table S4 in Supporting Information S1) however, the RMSDs for this region are much higher than SD, with the exception of algorithm-ESACCI salinity combination. Bates et al. (2005) found the Beaufort Sea to have highly variable DIC $<600\text{--}2,150 \mu\text{mol kg}^{-1}$ and results showed high seasonality. Tank et al. (2012) found a seasonally variable DIC flux from the Mackenzie River, the RiS_B region's largest river. Therefore, it is not surprising Arrigo et al. (2010) had the lowest uncertainties as this relationship takes into consideration the seasonal variability in primary productivity by incorporating Chl a into the algorithm, and by having two seasonal relationships it also captures the seasonal impact of fresh, riverine input. These results suggest that the algorithms are not robust enough to capture the nuances of the region (DeGrandpre et al., 2020) and need further development. There were too few matchups with the ESACCI data set in this region and we suggest continued effort to increase the number of in situ and satellite matchups. There are a larger number of data points in this region, which hopefully will allow algorithms to be developed further to improve the RMSD and bias.

4.5. Central Arctic

The TA algorithm-input combinations had the second highest uncertainties compared to other regions. It can therefore be deduced that TA algorithms-input combinations are not capturing the processes impacting TA in this region. Conditions are changing throughout the water column because of altered currents flowing into the CA, for example, saline Atlantic water is coming up from the deep ocean and is now found at shallower depths in the Eurasian Basin (Polyakov et al., 2017). Previous studies have found low TA values in the Makarov basin and the mean TA value from the OceanSODA-MDB was $2,041 \pm 131 \mu\text{mol kg}^{-1} \text{ year}^{-1}$, suggesting that this area may have low buffering capacity to additional CO_2 (Woosley & Millero, 2020). These changing conditions mean that algorithms will need regular updates. The changing water bodies will impact the TA algorithm uncertainties and could be one reason for the high uncertainties observed here. Further development is therefore important to use algorithms for monitoring TA here, as well as targeted DIC data collection to analyze and train algorithms as it is currently not possible for DIC in the CA.

5. Conclusions

Here we have demonstrated that the uncertainties of the algorithms and input combinations were observed to vary regionally across the Arctic Ocean, with all algorithm-input combinations having the lowest uncertainties in the AiS region and highest in the RiS regions. The results showed that TA algorithms-input combinations tended to have lower RMSD, and bias compared to DIC algorithms-input combinations. The algorithm-input combinations had low enough uncertainties in all regions with available data to distinguish natural variation for TA, but only in AiS, PiS and OFS is it possible to use these approaches to distinguish natural variation in DIC. The results showed that no algorithm-input combination consistently had the lowest uncertainties in all regions for both TA and DIC algorithms, highlighting the regionality of the Arctic Ocean. Though in situ re-analysis products had the lowest uncertainty with TA accuracy of $20.7 \mu\text{mol kg}^{-1}$ and bias of $2.3 \mu\text{mol kg}^{-1}$ in the AiS, satellite data also showed significant promise.

We consistently found the algorithm-satellite salinity combinations had much lower numbers of data points (n values), which is currently the main limitation to the use of satellite data. The low n values of satellite salinity data set matchups are in part due to the time span of the available satellite data, for instance SMOS satellite was only launched in 2010 and SMAP in 2015. Maintaining these and future satellite missions is therefore fundamental to increase the matchups and time-series. The other reason for low n values will be due to the small number of in situ data collected during periods of when satellites are overhead in their orbit. We therefore also recommend there is continued and enhanced effort for targeted in situ collection of TA and DIC data designed to support the use of satellite Arctic Ocean observations.

Future work should focus on developing these algorithms further to reduce bias and RMSD enabling the accurate identification of finer spatial scale changes. One improvement to the DIC algorithms could be made by updating

the algorithms to accommodate the DIC increase that has occurred since their development and then using this information within the algorithm training process or by including time in some other way. Further improvements could be made by estimating the surface residence time of ice-free waters. Future work should focus on developing these algorithms further to reduce bias and RMSD enabling the accurate identification of finer spatial scale changes of carbonate chemistry for the OA community. Notwithstanding these issues, the approaches used in this study could be used to evaluate the carbonate chemistry and OA conditions and history for Arctic Ocean organisms while informing experimental treatment levels within laboratory studies. Similarly, these data could be used to identify geographical refugia for some Arctic Ocean species.

Data Availability Statement

The matchup database “OceanSODA-MDB” which was used in the algorithm evaluation is available at <https://data-cersat.ifremer.fr/data/ocean-carbonate/oceansoda-mmdb/> (Land et al., 2023; Land & Piollé, 2022). The python code used to run the analysis can be found at <https://doi.org/10.5281/zenodo.10067204> (Green et al., 2023) and was adapted from DOI: <https://doi.org/10.5281/zenodo.10069611> (Sims et al., 2022).

References

- Anderson, L. G., Björk, G., Jutterström, S., Pipko, I., Shakhova, N., Semiletov, I., & Wählström, I. (2011). East Siberian Sea, an Arctic region of very high biogeochemical activity. *Biogeosciences*, 8(6), 1745–1754. <https://doi.org/10.5194/bg-8-1745-2011>
- Andreev, A. G., Chen, C. T. A., & Sereda, N. A. (2010). The distribution of the carbonate parameters in the waters of Anadyr Bay of the Bering Sea and in the western part of the Chukchi Sea. *Oceanology*, 50(1), 39–50. <https://doi.org/10.1134/S0001437010010054>
- Arrigo, K. R., Pabi, S., van Dijken, G. L., & Maslowski, W. (2010). Air-sea flux of CO₂ in the Arctic Ocean, 1998–2003. *Journal of Geophysical Research*, 115(G4), G04024. <https://doi.org/10.1029/2009JG001224>
- Banzon, V., Smith, T. M., Mike Chin, T., Liu, C., & Hankins, W. (2016). A long-term record of blended satellite and in situ sea-surface temperature for climate monitoring, modelling and environmental studies. *Earth System Science Data*, 8(1), 165–176. <https://doi.org/10.5194/essd-8-165-2016>
- Bates, N. R., Best, M. H. P., & Hansell, D. A. (2005). Spatio-temporal distribution of dissolved inorganic carbon and net community production in the Chukchi and Beaufort Seas. *Deep-Sea Research Part II: Topical Studies in Oceanography*, 52(24–26), 3303–3323. <https://doi.org/10.1016/j.dsr2.2005.10.005>
- Beaupré-Laperrière, A., Mucci, A., & Thomas, H. (2020). The recent state and variability of the carbonate system of the Canadian Arctic Archipelago and adjacent basins in the context of ocean acidification. *Biogeosciences*, 17(14), 3923–3942. <https://doi.org/10.5194/bg-17-3923-2020>
- Bellerby, R. G. J. (2017). Oceanography: Ocean acidification without borders. *Nature Climate Change*, 7(4), 241–242. <https://doi.org/10.1038/nclimate3247>
- Bellerby, R. G. J., Anderson, L. G., Osborne, E., Steiner, N., Pipko, I., Chieric, I., et al. (2018). Arctic Ocean acidification: An update. In *AMAP assessment 2018: Arctic Ocean acidification. Arctic monitoring and assessment programme (AMAP), Tromsø, Norway* (pp. 79–90). Retrieved from <https://www.amap.no/documents/doc/amap-assessment-2018-arctic-ocean-acidification/1659>
- Bellerby, R. G. J., Olsen, A., Furevik, T., & Anderson, L. A. (2005). Response of the surface ocean CO₂ system in the North Atlantic to climate change. In *Geophysical monograph series, AGU, (The Nordic Seas: An integrated perspective)*. <https://doi.org/10.1029/158GM13>
- Bienhold, C., Schourup-Kristensen, V., Krumpen, T., Nöthig, E. M., Wenzhöfer, F., Korhonen, M., et al. (2022). Effects of sea ice retreat and ocean warming on the Laptev Sea continental slope ecosystem (1993 vs 2012). *Frontiers in Marine Science*, 9(December), 1–26. <https://doi.org/10.3389/fmars.2022.1004959>
- BIPM. (2008). *Evaluation of measurement data — Guide to the expression of uncertainty in measurement* (Vol. 50) International Organization for Standardization. <https://doi.org/10.1373/clinchem.2003.030528>
- Boutin, J., Reul, N., Köhler, J., Martin, A., Catany, R., Guimbard, S., et al. (2021a). Satellite-based sea surface salinity designed for ocean and climate studies. *Journal of Geophysical Research: Oceans*, 126(11), e2021JC017676. <https://doi.org/10.1029/2021JC017676>
- Boutin, J., Vergely, J.-L., Reul, N., Catany, R., Köhler, J., Martin, A., et al. (2021b). *ESA sea surface salinity climate change initiative (Sea_Surface_Salinity_cci): Weekly sea surface salinity product, v03.21, for 2010 to 2020*. NERC EDS Centre for Environmental Data Analysis. Retrieved from <https://catalogue.ceda.ac.uk/uuid/fad2e982a59d44788eda09e3c67ed7d5>
- Boyer, T. P., Garcia, H. E., Locarnini, R. A., Zweng, M. M., Mishonov, A. V., Reagan, J. R., et al. (2018). World Ocean Atlas 2018 [Dataset]. NOAA National Centers for Environmental Information. <https://www.ncei.noaa.gov/archive/accession/NCEI-WOA18>
- Brewer, P. G., Glover, D. M., Goyet, C., & Shafer, D. K. (1995). The pH of the North Atlantic Ocean: Improvements to the global model for sound absorption in seawater. *Journal of Geophysical Research*, 100(C5), 8761–8776. <https://doi.org/10.1029/95JC00306>
- Brown, K. A., Holding, J. M., Carmack, E. C., & Cooper, L. W. (2020). Understanding regional and seasonal variability is key to gaining a pan-Arctic perspective on Arctic Ocean freshening. *Frontiers in Marine Science*, 7(August), 1–25. <https://doi.org/10.3389/fmars.2020.00606>
- Cabanes, C., Grouazel, A., Von Schuckmann, K., Hamon, M., Turpin, V., Coatanoan, C., et al. (2013). The CORA dataset: Validation and diagnostics of in-situ ocean temperature and salinity measurements. *Ocean Science*, 9(1), 1–18. <https://doi.org/10.5194/os-9-1-2013>
- Cai, Z., You, Q., Chen, H. W., Zhang, R., Chen, D., Chen, J., et al. (2022). Amplified wintertime Barents Sea warming linked to intensified Barents oscillation. *Environmental Research Letters*, 17(4), 044068. <https://doi.org/10.1088/1748-9326/ac5bb3>
- Caldeira, K., & Wickett, M. E. (2003). Anthropogenic carbon and ocean pH. *Nature*, 425(6956), 365. <https://doi.org/10.1038/425365a>
- Carmack, E., & Wassmann, P. (2006). Food webs and physical-biological coupling on pan-Arctic shelves: Unifying concepts and comprehensive perspectives. *Progress in Oceanography*, 71(2–4), 446–477. <https://doi.org/10.1016/j.pocean.2006.10.004>
- Cooper, L. W., McClelland, J. W., Holmes, R. M., Raymond, P. A., Gibson, J. J., Guay, C. K., & Peterson, B. J. (2008). Flow-weighted values of runoff tracers (δ18O, DOC, Ba, alkalinity) from the six largest Arctic rivers. *Geophysical Research Letters*, 35, L18606. <https://doi.org/10.1029/2008GL035007>
- Cross, J. N., Mathis, J. T., Pickart, R. S., & Bates, N. R. (2018). Formation and transport of corrosive water in the Pacific Arctic region. *Deep-Sea Research Part II*, 152(June), 67–81. <https://doi.org/10.1016/j.dsr2.2018.05.020>

- DeGrandpre, M., Evans, W., Timmermans, M. L., Krishfield, R., Williams, B., & Steele, M. (2020). Changes in the Arctic Ocean carbon cycle with diminishing ice cover. *Geophysical Research Letters*, *47*, e2020GL088051. <https://doi.org/10.1029/2020GL088051>
- DeGrandpre, M. D., Lai, C. Z., Timmermans, M. L., Krishfield, R. A., Proshutinsky, A., & Torres, D. (2019). Inorganic carbon and $p\text{CO}_2$ variability during ice formation in the Beaufort Gyre of the Canada Basin. *Journal of Geophysical Research: Oceans*, *124*(6), 4017–4028. <https://doi.org/10.1029/2019JC015109>
- Dickson, A. G., Sabine, C. L., & Christian, J. R. (Eds.) (2007). *Guide to best practices for ocean CO_2 measurements* (p. 191). PICES Special Publication 3.
- Drake, T. W., Tank, S. E., Zhulidov, A. V., Holmes, R. M., Gurtovaya, T., & Spencer, R. G. M. (2018). Increasing alkalinity export from large Russian Arctic rivers. *Environmental Science and Technology*, *52*(15), 8302–8308. <https://doi.org/10.1021/acs.est.8b01051>
- Findlay, H. S., Gibson, G., Kędra, M., Morata, N., Pavlov, A. K., Reigstad, M., et al. (2015). Responses in Arctic marine carbon cycle processes: Conceptual scenarios and implications for ecosystem function. *Polar Research*, *34*(1), 24252. <https://doi.org/10.3402/polar.v34.24252>
- Fine, R. A., Willey, D. A., & Millero, F. J. (2017). Global variability and changes in ocean total alkalinity from Aquarius satellite data. *Geophysical Research Letters*, *44*(1), 261–267. <https://doi.org/10.1002/2016GL07171>
- Ford, D., Tilstone, G. H., Shutler, J. D., Kitidis, V., Lobanova, P., Schwarz, J., et al. (2021). Wind speed and mesoscale features drive net autotrophy in the South Atlantic Ocean. *Remote Sensing of Environment*, *260*(July 2020), 112435. <https://doi.org/10.1016/j.rse.2021.112435>
- Fransner, F., Fröb, F., Tjiputra, J., Goris, N., Lauvset, S. K., Skjelvan, I., et al. (2022). Acidification of the Nordic Seas. *Biogeosciences*, *19*(3), 979–1012. <https://doi.org/10.5194/bg-19-979-2022>
- Fransson, A., Chierici, M., Anderson, L. G., Bussman, I., Kattner, G., Jones, E. P., & Swift, J. H. (2001). The importance of shelf processes for the modification of chemical constituents in the waters of the eastern Arctic Ocean. *Continental Shelf Research*, *21*(3), 225–242. [https://doi.org/10.1016/S0278-4343\(00\)00088-1](https://doi.org/10.1016/S0278-4343(00)00088-1)
- Friedlingstein, P., Jones, M. W., Sullivan, M. O., Andrew, R. M., Bakker, C. E., Hauck, J., et al. (2021). Global carbon budget 2021. *Earth System Science Data*, *14*, 1917–2005. <https://doi.org/10.5194/essd-14-1917-2022>
- Geilfus, N. X., Munson, K., Lemes, M., Wang, F., Tison, J. L., & Rysgaard, S. (2021). Meteoric water contribution to sea ice formation and its control of the surface water carbonate cycle on the Wandel Sea shelf, northeastern Greenland. *Elementa*, *9*(1), 1–19. <https://doi.org/10.1525/elementa.2021.00004>
- Good, S. A., Embury, O., Bulgin, C. E., & Mittaz, J. (2019). ESA Sea Surface Temperature Climate Change Initiative (SST_cci): Level 4 analysis climate data record version 2.1 [Dataset]. Centre for Environmental Data Analysis. <https://doi.org/10.5285/62c0f97b1eac4e0197a674870afe1ee6>
- Good, S., Fiedler, E., Mao, C., Martin, M. J., Maycock, A., Reid, R., et al. (2020). The current configuration of the OSTIA system for operational production of foundation sea surface temperature and ice concentration analyses. *Remote Sensing*, *12*(4), 1–20. <https://doi.org/10.3390/rs12040720>
- Green, H. L., Sims, R., Holding, T., Land, P., & Shutler, J. (2023). Observing temporally varying synoptic-scale total alkalinity and dissolved inorganic carbon in the Arctic Ocean (Arctic_Ocean_OceanSODA 1.0) [Code]. Zenodo. <https://doi.org/10.5281/zenodo.10067204>
- Green, H. L., Findlay, H. S., Shutler, J. D., Land, P. E., & Bellerby, R. G. J. (2021). Satellite Observations are needed to understand ocean acidification and multi-stressor impacts on fish stocks in a changing Arctic Ocean. *Frontiers in Marine Science*, *8*(June), 1–8. <https://doi.org/10.3389/fmars.2021.635797>
- Gregor, L., & Gruber, N. (2021). OceanSODA-ETHZ: A global gridded data set of the surface ocean carbonate system for seasonal to decadal studies of ocean acidification. *Earth System Science Data*, *13*(2), 777–808. <https://doi.org/10.5194/essd-13-777-2021>
- Huang, B., Liu, C., Banzon, V., Freeman, E., Graham, G., Hankins, B., et al. (2021). Improvements of the Daily Optimum Interpolation Sea Surface Temperature (DOISST) Version 2.1. *Journal of Climate*, *34*(8), 2923–2939. <https://doi.org/10.1175/JCLI-D-20-0166.1>
- Jones, E. M., Chierici, M., Menze, S., Fransson, A., Ingvaldsen, R. B., & Lødemel, H. H. (2021). Ocean acidification state variability of the Atlantic Arctic Ocean around northern Svalbard. *Progress in Oceanography*, *199*, 102708. <https://doi.org/10.1016/j.pocean.2021.102708>
- Jutterström, S., & Anderson, L. G. (2010). Uptake of CO_2 by the Arctic Ocean in a changing climate. *Marine Chemistry*, *122*(1–4), 96–104. <https://doi.org/10.1016/j.marchem.2010.07.002>
- Kaltin, S., & Anderson, L. G. (2005). Uptake of atmospheric carbon dioxide in Arctic shelf seas: Evaluation of the relative importance of processes that influence $p\text{CO}_2$ in water transported over the Bering-Chukchi Sea shelf. *Marine Chemistry*, *94*(1–4), 67–79. <https://doi.org/10.1016/j.marchem.2004.07.010>
- Kaltin, S., Anderson, L. G., Olsson, K., Fransson, A., & Chierici, M. (2002). Uptake of atmospheric carbon dioxide in the Barents Sea. *Journal of Marine Systems*, *38*(1–2), 31–45. [https://doi.org/10.1016/S0924-7963\(02\)00168-9](https://doi.org/10.1016/S0924-7963(02)00168-9)
- Kim, D., Yang, E. J., Cho, S., Kim, H. J., Cho, K. H., Jung, J., & Kang, S. H. (2021). Spatial and temporal variations of aragonite saturation states in the surface waters of the western Arctic Ocean. *Journal of Geophysical Research: Oceans*, *126*(11), 1–13. <https://doi.org/10.1029/2021JC017738>
- Kolodziejczyk, N., Hamon, M., Boutin, J., Vergely, J.-L., Reverdin, G., Supply, A., & Reul, N. (2021). Objective analysis of SMOS and SMAP sea surface salinity to reduce large-scale and time-dependent biases from low to high latitudes. *Journal of Atmospheric and Oceanic Technology*, *38*(3), 405–421. <https://doi.org/10.1175/JTECH-D-20-0093.1>
- Kolodziejczyk, N., Prigent-Mazella, A., & Gaillard, F. (2021). ISAS temperature and salinity gridded fields [Dataset]. SEANOE. <https://doi.org/10.17882/52367>
- Krasting, J. P., De Palma, M., Sonnewald, M., Dunne, J. P., & John, J. G. (2022). Regional sensitivity patterns of Arctic Ocean acidification revealed with machine learning. *Nature Communications Earth and Environment*, *3*, 1–11. <https://doi.org/10.1038/s43247-022-00419-4>
- Kwok, R. (2018). Arctic sea ice thickness, volume, and multiyear ice coverage: Losses and coupled variability (1958–2018). *Environmental Research Letters*, *13*(10), 105005. <https://doi.org/10.1088/1748-9326/aae3ec>
- Land, P. E., Findlay, H. S., Shutler, J. D., Ashton, I. G. C., Holding, T., Grouazel, A., et al. (2019). Remote Sensing of Environment Optimum satellite remote sensing of the marine carbonate system using empirical algorithms in the global ocean, the Greater Caribbean, the Amazon Plume and the Bay of Bengal. *Remote Sensing of Environment*, *235*(February), 111469. <https://doi.org/10.1016/j.rse.2019.111469>
- Land, P. E., Findlay, H. S., Shutler, J. D., Piolle, J., Sims, R., Green, H. L., et al. (2023). OceanSODA-MDB: A standardised surface ocean carbonate system dataset for model-data intercomparisons. *Earth System Science Data*, *15*, 921–947. <https://doi.org/10.5194/essd-15-921-2023>
- Land, P. E., & Piolle, J. (2022). OceanSODA standardised surface ocean carbonate system matchup dataset (3.4), IFREMER, France [Dataset]. <https://doi.org/10.12770/0dc16d62-05f6-4bbe-9dc4-6d47825a5931>
- Land, P. E., Shutler, J. D., Findlay, H. S., Girard-Arduin, F., Sabia, R., Reul, N., et al. (2015). Salinity from space unlocks satellite-based assessment of ocean acidification. *Environmental Science and Technology*, *49*(4), 1987–1994. <https://doi.org/10.1021/es504849s>
- Lee, K., Tong, L. T., Millero, F. J., Sabine, C. L., Dickson, A. G., Goyet, C., et al. (2006). Global relationships of total alkalinity with salinity and temperature in surface waters of the world's oceans. *Geophysical Research Letters*, *33*(19), 1–5. <https://doi.org/10.1029/2006GL027207>

- Lee, K., Wanninkhof, R., Feely, R. A., Millero, F. J., & Peng, T. H. (2000). Global relationships of total inorganic carbon with temperature and nitrate in surface seawater. *Global Biogeochemical Cycles*, *14*(3), 979–994. <https://doi.org/10.1029/1998GB001087>
- Lewis, K. M., Mitchell, B. G., van Dijken, G. L., & Arrigo, K. R. (2016). Regional chlorophyll a algorithms in the Arctic Ocean and their effect on satellite-derived primary production estimates. *Deep-Sea Research Part II: Topical Studies in Oceanography*, *130*, 14–27. <https://doi.org/10.1016/j.dsr2.2016.04.020>
- Li, S., Lin, P., Dou, T., Xiao, C., Itoh, M., Kikuchi, T., & Qin, D. (2022). Upwelling of Atlantic water in Barrow Canyon, Chukchi Sea. *Journal of Geophysical Research: Oceans*, *127*(3), 1–19. <https://doi.org/10.1029/2021jc017839>
- Lind, S., Ingvaldsen, R. B., & Furevik, T. (2018). Arctic warming hotspot in the northern Barents Sea linked to declining sea-ice import. *Nature Climate Change*, *8*(7), 634–639. <https://doi.org/10.1038/s41558-018-0205-y>
- MacGilchrist, G. A., Naveira Garabato, A. C., Tsubouchi, T., Bacon, S., Torres-Valdés, S., & Azetsu-Scott, K. (2014). The Arctic Ocean carbon sink. *Deep-Sea Research Part I: Oceanographic Research Papers*, *86*, 39–55. <https://doi.org/10.1016/j.dsr.2014.01.002>
- Mathis, J. T., & Questel, J. M. (2013). Assessing seasonal changes in carbonate parameters across small spatial gradients in the Northeastern Chukchi Sea. *Continental Shelf Research*, *67*, 42–51. <https://doi.org/10.1016/j.csr.2013.04.041>
- Meissner, T., & Wentz, F. J. (2019). *Remote sensing systems SMAP ocean surface salinities, Version 4.0 validated release*. Remote Sensing Systems.
- Merchant, C. J., Embury, O., Bulgina, C. E., Block, T., Corlett, G. K., Fiedler, E., et al. (2019). Satellite-based time-series of sea-surface temperature since 1981 for climate applications. *Scientific Data*, *6*, 1–18. <https://doi.org/10.1038/s41597-019-0236-x>
- Millero, F. J., Lee, K., & Roche, M. (1998). Distribution of alkalinity in the surface waters of the major oceans. *Marine Chemistry*, *60*(1–2), 111–130. [https://doi.org/10.1016/S0304-4203\(97\)00084-4](https://doi.org/10.1016/S0304-4203(97)00084-4)
- Nondal, G., Bellerby, R. G. J., Olsen, A., Johannessen, T., & Olafsson, J. (2009). Optimal evaluation of the surface ocean CO₂ system in the northern North Atlantic using data from voluntary observing ships. *Limnology and Oceanography: Methods*, *7*(1), 109–118. <https://doi.org/10.4319/lom.2009.7.109>
- Olmedo, E., Gabarró, C., González-Gambau, V., Martínez, J., Ballabrera-Poy, J., Turiel, A., et al. (2018). Seven years of SMOS sea surface salinity at high latitudes: Variability in Arctic and Sub-Arctic Regions. *Remote Sensing*, *10*(11), 1–24. <https://doi.org/10.3390/rs10111772>
- Onarheim, I. H., & Árhun, M. (2017). Toward an ice-free Barents Sea. *Geophysical Research Letters*, *44*(16), 8387–8395. <https://doi.org/10.1002/2017GL074304>
- Oziel, L., Baudena, A., Ardyna, M., Massicotte, P., Randelhoff, A., Sallée, J. B., et al. (2020). Faster Atlantic currents drive poleward expansion of temperate phytoplankton in the Arctic Ocean. *Nature Communications*, *11*(1), 1–8. <https://doi.org/10.1038/s41467-020-15485-5>
- Patterson, T., & Vaughn Kelso, N. (2023). Natural earth. Retrieved from <https://www.naturalearthdata.com/>
- Pipko, I. I., Pugach, S. P., & Semiletov, I. P. (2016). Assessment of the CO₂ fluxes between the ocean and the atmosphere in the eastern part of the Laptev Sea in the ice-free period. *Doklady Earth Sciences*, *467*(2), 398–401. <https://doi.org/10.1134/S1028334X16040127>
- Pogojeva, M., Polukhin, A., Makkaveev, P., Staalstrøm, A., Berezina, A., & Yakushev, E. (2022). Arctic inshore biogeochemical regime influenced by coastal runoff and glacial melting (case study for the Templefjord, Spitsbergen). *Geosciences (Switzerland)*, *12*(1), 44. <https://doi.org/10.3390/geosciences12010044>
- Polyakov, I. V., Pnyushkov, A. V., Alkire, M. B., Ashik, I. M., Baumann, T. M., Carmack, E. C., et al. (2017). Greater role for Atlantic inflows on sea-ice loss in the Eurasian Basin of the Arctic Ocean. *Science*, *356*(6335), 285–291. <https://doi.org/10.1126/science.aai8204>
- Qi, D., Chen, L., Chen, B., Gao, Z., Zhong, W., Feely, R. A., et al. (2017). Increase in acidifying water in the western Arctic Ocean. *Nature Climate Change*, *7*(February), 195–199. <https://doi.org/10.1038/NCLIMATE3228>
- Qi, D., Wu, Y., Chen, L., Cai, W., Ouyang, Z., Zhang, Y., et al. (2022). Rapid acidification of the Arctic Chukchi sea waters driven by anthropogenic forcing and biological carbon recycling. *Geophysical Research Letters*, *49*(4). <https://doi.org/10.1029/2021GL097246>
- Quillen, Y., Shutler, J., Piolle, J. F., & Autret, E. (2021). Recent trends in the wind-driven California current upwelling system. *Remote Sensing of Environment*, *261*(September 2020), 112486. <https://doi.org/10.1016/j.rse.2021.112486>
- Robertson, J. E., Robinson, C., Turner, D. R., Holligan, P., Watson, A. J., Boyd, P., et al. (1994). The impact of a coccolithophore bloom on oceanic carbon uptake in the northeast Atlantic during summer 1991. *Deep-Sea Research Part I*, *41*(2), 297–314. [https://doi.org/10.1016/0967-0637\(94\)90005-1](https://doi.org/10.1016/0967-0637(94)90005-1)
- Salisbury, J., Vandemark, D., Jönsson, B., Balch, W., Chakraborty, S., Lohrenz, S., et al. (2015). How can present and future satellite missions support scientific studies that address ocean acidification? *Oceanography*, *25*(2), 108–121. <https://doi.org/10.5670/oceanog.2015.35>
- Sathyendranath, S., Brewin, R. J. W., Brockmann, C., Brotas, V., Calton, B., Chuprin, A., et al. (2019). An ocean-colour time series for use in climate studies: The experience of the ocean-colour climate. *Sensors*, *19*(October), 4285. <https://doi.org/10.3390/s19194285>
- Semiletov, I., Pipko, I., Gustafsson, Ö., Anderson, L. G., Sergienko, V., Pugach, S., et al. (2016). Acidification of East Siberian Arctic Shelf waters through addition of freshwater and terrestrial carbon. *Nature Geoscience*, *9*(5), 361–365. <https://doi.org/10.1038/ngeo2695>
- Semiletov, I. P., Pipko, I. I., Repina, I., & Shakhova, N. E. (2007). Carbonate chemistry dynamics and carbon dioxide fluxes across the atmosphere-ice-water interfaces in the Arctic Ocean: Pacific sector of the Arctic. *Journal of Marine Systems*, *66*(1–4), 204–226. <https://doi.org/10.1016/j.jmarsys.2006.05.012>
- Shiklomanov, A., Déry, S., Tretiakov, M., Yang, D., Magritsky, D., Georgiadi, A., & Tang, W. (2021). *River freshwater flux to the Arctic Ocean. Arctic hydrology, permafrost and ecosystems*. Springer International Publishing. <https://doi.org/10.1007/978-3-030-50930-9>
- Shutler, J. D., Wanninkhof, R., Nightingale, P. D., Woolf, D. K., Bakker, D. C. E., Watson, A., et al. (2020). Satellites will address critical science priorities for quantifying ocean carbon. *Frontiers in Ecology and the Environment*, *18*, 1–9. <https://doi.org/10.1002/fee.2129>
- Sims, R. P., Holding, T., Land, P. E., Piolle, J.-F., Green, H., & Shutler, J. D. (2022). JamieLab/OceanSODA: v1.1.0 (v1.1.0) [Code]. Zenodo. <https://doi.org/10.5281/zenodo.10069611>
- Sims, R. P., Holding, T. M., Land, P. E., Piolle, J., Green, H. L., & Shutler, J. D. (2023). OceanSODA-UNEXE: A multi-year gridded Amazon and Congo River outflow surface ocean carbonate system dataset. *Earth System Science Data*, *1*, 1–32. <https://doi.org/10.5194/essd-2022-294>
- Skjelvan, I., Lauvset, S. K., Johannessen, T., Gundersen, K., & Skagseth, Ø. (2022). Decadal trends in Ocean acidification from the ocean weather station M in the Norwegian Sea. *Journal of Marine Systems*, *234*(June), 103775. <https://doi.org/10.1016/j.jmarsys.2022.103775>
- Solomon, A., Heuzé, C., Rabe, B., Bacon, S., Bertino, L., Heimbach, P., et al. (2021). Freshwater in the Arctic Ocean 2010–2019. *Ocean Science*, *17*(4), 1081–1102. <https://doi.org/10.5194/os-17-1081-2021>
- Swift, C. T., & McIntosh, R. E. (1983). Considerations for microwave remote sensing of ocean-surface salinity. *IEEE Transactions on Geoscience and Remote Sensing*, *21*(4), 480–491. <https://doi.org/10.1109/TGRS.1983.350511>
- Szekely, T., Gourrion, J., Pouliquen, S., & Reverdin, G. (2019). The CORA 5.2 dataset for global in situ temperature and salinity measurements: Data description and validation. *Ocean Science*, *15*(6), 1601–1614. <https://doi.org/10.5194/os-15-1601-2019>
- Szekely, T., Gourrion, J., Pouliquen, S., Reverdin, G., & Mercœur, F. (2019). CORA, coriolis ocean dataset for reanalysis. <https://doi.org/10.17882/46219>

- Tait, V. K., Gershey, R. M., & Jones, E. P. (2000). Inorganic carbon in the Labrador Sea: Estimation of the anthropogenic component. *Deep-Sea Research Part I: Oceanographic Research Papers*, 47(2), 295–308. [https://doi.org/10.1016/S0967-0637\(99\)00059-X](https://doi.org/10.1016/S0967-0637(99)00059-X)
- Takahashi, T., Sutherland, S. C., Chipman, D. W., Goddard, J. G., Ho, C., Newberger, T., et al. (2014). Climatological distributions of pH, pCO₂, total CO₂, alkalinity, and CaCO₃ saturation in the global surface ocean, and temporal changes at selected locations. *Marine Chemistry*, 164, 95–125. <https://doi.org/10.1016/j.marchem.2014.06.004>
- Tank, S. E., Raymond, P. A., Striegl, R. G., McClelland, J. W., Holmes, R. M., Fiske, G. J., & Peterson, B. J. (2012). A land-to-ocean perspective on the magnitude, source and implication of DIC flux from major Arctic rivers to the Arctic Ocean. *Global Biogeochemical Cycles*, 26(4), 1–15. <https://doi.org/10.1029/2011GB004192>
- Tynan, E., Clarke, J. S., Humphreys, M. P., Ribas-Ribas, M., Esposito, M., Rérolle, V. M. C., et al. (2016). Physical and biogeochemical controls on the variability in surface pH and calcium carbonate saturation states in the Atlantic sectors of the Arctic and Southern Oceans. *Deep-Sea Research Part II: Topical Studies in Oceanography*, 127, 7–27. <https://doi.org/10.1016/j.dsr2.2016.01.001>
- Ulfso, A., Rabe, B., Jones, E. M., Karcher, M., Casacuberta, N., Korhonen, M., & van Heuven, S. M. A. C. (2018). Rapid changes in anthropogenic carbon storage and ocean acidification in the intermediate layers of the Eurasian Arctic Ocean: 1996–2015. *Global Biogeochemical Cycles*, 32(9), 1254–1275. <https://doi.org/10.1029/2017gb005738>
- Vinogradova, N., Lee, T., Boutin, J., Drushka, K., Fournier, S., Sabia, R., et al. (2019). Satellite salinity observing system: Recent discoveries and the way forward. *Frontiers in Marine Science*, 6, 243. <https://doi.org/10.3389/fmars.2019.00243>
- Wassmann, P., Reigstad, M., Haug, T., Rudels, B., Carroll, M. L., Hop, H., et al. (2006). Food webs and carbon flux in the Barents Sea. *Progress in Oceanography*, 71(2–4), 232–287. <https://doi.org/10.1016/j.pocean.2006.10.003>
- Wong, C. S., Waser, N. A. D., Nojiri, Y., Whitney, F. A., Page, J. S., & Zeng, J. (2002). Seasonal cycles of nutrients and dissolved inorganic carbon at high and mid latitudes in the North Pacific Ocean during the Skaugran cruises: Determination of new production and nutrient uptake ratios. *Deep-Sea Research Part II: Topical Studies in Oceanography*, 49(24–25), 5317–5338. [https://doi.org/10.1016/S0967-0645\(02\)00193-5](https://doi.org/10.1016/S0967-0645(02)00193-5)
- Woosley, R. J., & Millero, F. J. (2020). Freshening of the western Arctic negates anthropogenic carbon uptake potential. *Limnology and Oceanography*, 65(8), 1–13. <https://doi.org/10.1002/lno.11421>
- Yamamoto-Kawai, M., McLaughlin, F. A., Carmack, E. C., Nishino, S., & Shimada, K. (2009). Aragonite undersaturation in the Arctic. *Science*, 326(November), 1098–1100. <https://doi.org/10.1126/science.1174190>
- Yueh, S. H., West, R., Wilson, W. J., Li, F. K., Njoku, E. G., & Rahmat-Samii, Y. (2001). Error sources and feasibility for microwave remote sensing of ocean surface salinity. *IEEE Transactions on Geoscience and Remote Sensing*, 39(5), 1049–1060. <https://doi.org/10.1109/36.921423>
- Zhang, Y., Yamamoto-Kawai, M., & Williams, W. J. (2020). Two decades of ocean acidification in the surface waters of the Beaufort Gyre, Arctic Ocean: Effects of sea ice melt and retreat from 1997–2016. *Geophysical Research Letters*, 47(3), 1–11. <https://doi.org/10.1029/2019GL086421>